# Infrared Photodissociation Spectroscopy of Electrosprayed Ions in a Fourier Transform Mass Spectrometer

**ARTICLE** *in* JOURNAL OF THE AMERICAN CHEMICAL SOCIETY · APRIL 2005

Impact Factor: 12.11 · DOI: 10.1021/ja040136n · Source: PubMed



**8 AUTHORS**, INCLUDING:

Han Bin Oh
Sogang University
**52** PUBLICATIONS **535** CITATIONS

SEE PROFILE

J|A|C|S
ARTICLES
Published on Web 02/24/2005

# Infrared Photodissociation Spectroscopy of Electrosprayed Ions in a Fourier Transform Mass Spectrometer

Han-Bin Oh,[†] Cheng Lin,[‡] Harold Y. Hwang,[‡] Huili Zhai,[‡] Kathrin Breuker,[§] Vladimir Zabrouskov,[‡] Barry K. Carpenter,[‡] and Fred W. McLafferty*[,‡]

*Contribution from the Department of Chemistry, Sogang University, Seoul 121-742, South Korea, Department of Chemistry and Chemical Biology, Cornell University, Ithaca 14853-1301, New York, and Institute of Organic Chemistry, University of Innsbruck, Innrain 52a, 6020 Innsbruck, Austria*

Received May 15, 2004; E-mail: fwm5@cornell.edu

***Abstract:*** Previous gas-phase methods for infrared photodissociation spectroscopy (IRPD) require sample volatility. Our method instead uses electrospray ionization to introduce even large nonvolatile molecules into a Fourier transform mass spectrometer, where extended (>15 s) ion storage makes possible high sensitivity spectral measurements with an OPO laser over a range of 3050−3800 $cm^{-1}$. The spectra of 22 gaseous proton-bound amino acid complexes are generally correlated with the H-stretching frequencies established for O−H and N−H functional groups in solution. For theoretical structure predictions of the $Gly_2H^+$ and N-acylated $Asp_2H^+$ dimers, IRPD spectra clearly differentiate between the predicted lowest energy conformers. In contrast to solution, in the gas phase the glycine zwitterion is ∼20 kcal/mol less stable than the neutral; however, glycine is clearly zwitterionic in the gaseous $GlyLysH^+$ dimer. The level of theory is inadequate for the larger $Lys_2H^+$ dimer, as all low energy predicted structures have free carboxyl O−H groups, in contrast to the IR spectrum. IRPD appears to be a promising new technique for providing unique information on a broad range of biomolecular and other gaseous ions, especially on noncovalent bonding involving O−H and N−H groups.

## Introduction

For fundamental biological processes such as protein folding and enzyme/substrate binding, the complete removal of solvent provides a unique opportunity to characterize the effect of solvation on intra- or intermolecular noncovalent bonding.[1−4] A variety of spectroscopic methods have been used to study gaseous biomolecules, both as neutrals[1] and as ions,[2,3] but these species had to have the stability and vapor pressure appropriate for sampling methods such as supersonic free jet expansion, electron ionization (EI), and corona discharge.[1−3] In a recent preliminary communication,[5] we showed that electrospray ionization (ESI)[6] makes possible the application of classical infrared spectroscopy (3050−3800 $cm^{-1}$) to samples as large as ubiquitin (8.6 kDa) by photodissociation of the resulting ions stored in a Fourier transform (FT) mass spectrometer; this instrument has been used previously to measure 925−1090 $cm^{-1}$ spectra of small EI molecular ions.[2] Here, the fundamentals of this methodology are established and its spectra (Figure 1) are used to characterize the molecular structures of 22 proton-bound amino acid dimers and multimers with the aid of theoretical predictions. Continuing to refer to this method as infrared photodissociation (IRPD) spectroscopy[3] is preferable to distinguish it from the common fixed wavelength technique for

[†] Sogang University.
[‡] Cornell University.
[§] University of Innsbruck.

(1) (a) Rizzo, T. R.; Park, Y. D.; Levy, D. H. *J. Chem. Phys*. **1986**, *85*, 6945−6951. (b) Chapo, C. N.; Paul, J. B.; Provencal, R. A.; Roth, K.; Saykally, R. J. *J. Am. Chem. Soc*. **1998**, *120*, 12956−12957. (c) Robertson, E. G.; Simons, J. P. *Phys. Chem. Chem. Phys*. **2001**, *3*, 1−18. (d) Snoek, L. C.; Kroemer, R. T.; Simons, J. P. *Phys. Chem. Chem. Phys*. **2002**, *4*, 2130−2139. (e) Dian, B. C.; Longarte, A.; Zwier, T. S. *Science* **2002**, *296*, 2369−2273. (f) Roscioli, J. R.; Pratt, D. W. *Proc. Natl. Acad. Sci. U.S.A.* **2003**, *100*, 13752−13754.

(2) (a) Woodin, R. L.; Bomse, D. S.; Beauchamp, J. L. *J. Am. Chem. Soc*. **1978**, *100*, 3248−3250. (b) Miller, T. A.; Bondybey, V. A. *Molecular Ions: Spectroscopy, Structure, and Chemistry*; North-Holland Publishing: Amsterdam, 1983. (c) Thorne, L. R.; Beauchamp, J. L. Infrared Photochemistry of Gas-Phase Ions. In *Gas Phase Ion Chemistry*; Bowers, M. T., Ed.; Academic Press: New York, 1984; Vol. 3, pp 41−97. (d) Peiris, D. M.; Cheeseman, M. A.; Ramanathan, R.; Eyler, J. R. *J. Phys. Chem*. **1993**, *97*, 7839−7843.

(3) (a) Yeh, L. I.; Okumura, M.; Myers, J. D.; Price, J. M.; Lee, Y. T. *J. Chem. Phys*. **1989**, *91*, 7319−7330. (b) Wang, Y.-S.; Chang, H.-C.; Jiang, J.-C.; Lin, S. H.; Lee, Y. T.; Chang, H.-C. *J. Am. Chem. Soc*. **1998**, *120*, 8777−8788. (c) Jiang, J.-Y.; Wang, Y.-S.; Chang, H.-C.; Lin, S. H.; Lee, Y. T.; Niedner-Schatterburg, G.; Chang, H.-C. *J. Am. Chem. Soc*. **2000**, *122*, 1398−1410. (d) Wu, C.-C.; Jiang, J.-C.; Hahndorf, I.; Chaudhuri, C.; Lee, Y. T.; Chang, H.-C. *J. Phys. Chem. A* **2000**, *104*, 9556−9565. (e) Woo, C.-C.; Jiang, J. C.; Boo, D. W.; Lin, S. H.; Lee, Y. T.; Chang, H.-C. *J. Chem. Phys*. **2000**, *112*, 176−188. (f) Wang, Y. S.; Tsai, C. H.; Lee, Y. T.; Chang, H.-C.; Jiang, J. C.; Asvany, O.; Schlemmer, S.; Gerlich, D. *J. Phys. Chem. A* **2003**, *107*, 4217−4225. (g) Solca, N.; Dopfer, O. *J. Am. Chem. Soc*. **2004**, *126*, 9520−9521 and references therein.

(4) (a) Suckau, D.; Shi, Y.; Beu, S. C.; Senko, M. W.; Quinn, J. P.; Wampler, F. M., III; McLafferty, F. W. *Proc. Natl. Acad. Sci. U.S.A.* **1993**, *90*, 790−793. (b) Wyttenbach, T.; von Helden, G. J. E.; Bowers, M. T. *J. Am. Chem. Soc*. **1996**, *118*, 8355−8364. (c) McLafferty, F. W.; Guan, Z.; Haupts, U.; Wood, T. D.; Kelleher, N. L. *J. Am. Chem. Soc*. **1998**, *120*, 4732−4740. (d) Hoaglund-Hyzer, C. S.; Counterman, A. E.; Clemmer, D. E. *Chem. Rev*. **1999**, *99*, 3037−3079.

(5) Oh, H.-B.; Breuker, K.; Sze, S. K.; Ge, Y.; Carpenter, B. K.; McLafferty, F. W. *Proc. Natl. Acad. Sci. U.S.A.* **2002**, *99*, 15863−15868.

(6) Fenn, J. B.; Mann, M.; Meng, C. K.; Wong, S. F.; Whitehouse, C. M. *Science* **1989**, *246*, 64−71.


**10.1021/ja040136n CCC: $30.25** 

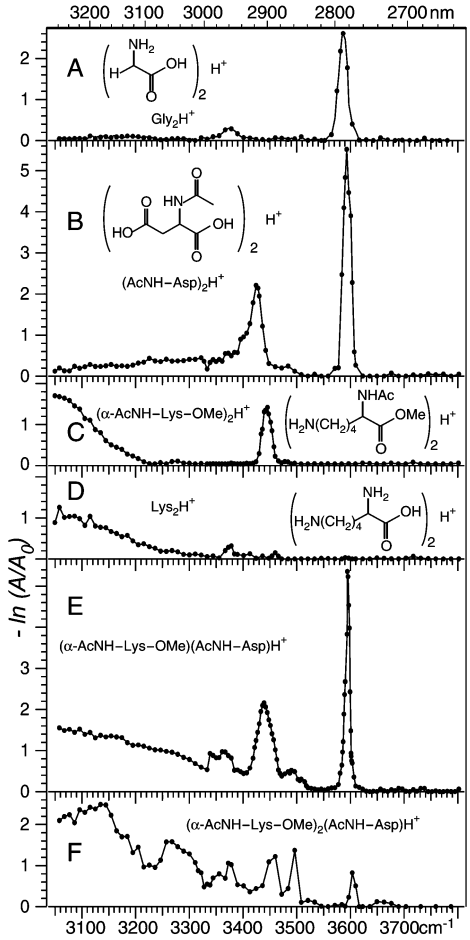


***Figure 1.*** IRPD spectra of proton-bound amino acid dimers and trimers at 27 °C, measured as depletion of the molecular ion abundance versus frequency. The depletion was the result of 15 s of IR irradiation (10 Hz repetition rate), normalized to the OPO laser tuning curve.

tandem mass spectrometry, infrared multiphoton dissociation (IRMPD).[7]

IRPD in the 2700−3900 $cm^{-1}$ region, combined with theory, has provided definitive O−H and N−H bonding information on small $H^+$-bound cluster ions such as $(H_2O)_{2-8}H^+$ and $(H_2O)_{3-6}NH_4^+$.[3a−f] Recent similar IRPD spectra use O−H absorptions to characterize protonated ethanol dimer by dissociating its $N_2$ gas adducts.[3g] Exciting recent studies[8] use the free electron laser[9] to measure spectra in the 600−2100 $cm^{-1}$ region, such as the fundamental vibrations of $H^+$ in $(H_2O)_2H^+$.[8a]

The gaseous amino acid dimers studied here represent more complex proton-bound systems. Such ions have been the subject of extensive basic research using a variety of mass spectrometry (MS) methods, in particular those for the determination of proton affinities and bond dissociation energies.[10] Of special recent interest are structural effects on the competitive charging of heteroatoms;[11] conditions for the stabilization of zwitterions in the gas-phase remain debatable.[1b,11a,d] For example, although the glycine zwitterion is stable in solution, in the gas phase it is unstable by ∼20 kcal/mol.[10a] As novel experimental data for the characterization of such systems, the 3050−3800 $cm^{-1}$ absorptions measured here by IRPD reflect the O−H and N−H structural environment, with both hydrogen bonding and charging on the heteroatom causing characteristic spectral red shifts. For simple ions, theory has provided useful predictions of the lowest energy conformational structures as well as their expected IR absorption frequencies;[3,12,13] this will be tested here with more complex ions. The spectra/structure relations established here will be applied to the IRPD spectra of multiply charged ubiquitin[5] and other protein ions in a later paper.[14]

## Experimental and Theoretical Methods

Experiments were performed on a 6T FT ion cyclotron resonance MS instrument described previously.[4c,5] Ions were formed from samples (Sigma, St. Louis, MO) by ESI (1−5 mM solutions in 49:49:2 $H_2O$:MeOH:AcOH), transported through three quadrupole RF-only ion guides, and trapped in the ion cell with a $N_2$ gas pulse (∼$10^{-6}$ Torr). The desired ions were mass selected using stored waveform inverse Fourier transform (SWIFT) waveforms[15] and were stored in the ion cell for >15 s to achieve ∼$10^{-9}$ Torr pressure and thermal equilibration.

IR radiation, tunable from 3050 to 3800 $cm^{-1}$ and line width ∼5 $cm^{-1}$ (factory calibrated as 3−4 $cm^{-1}$), was produced by an OPO system (IR OPO 2732, OPOTek, Carlsbad, CA) pumped by a Nd:YAG laser (Quantel S. A., France), pulse energy 6−10 mJ in 4 ns. With assembly as in Figure 2, the laser beam diameter in the ion cell is ∼1 mm. The laser repetition rate was adjusted (1−10 Hz) by changing the Q-switch frequency, the irradiation time was controlled by a mechanical shutter

(7) Little, D. P.; Speir, J. P.; Senko, M. W.; O'Connor, P. B.; McLafferty, F. W. *Anal. Chem.* **1994**, *66*, 2809−2815.
(8) (a) Asmis, K. R.; Pivonka, N. L.; Santambrogio, G.; Brümmer, M.; Kaposta, C.; Neumark, D. M.; Wöste, L. *Science* **2003**, *299*, 1375−1377. (b) Oomens, J.; Moore, D. T.; von Helden, G.; Meijer, G.; Dunbar, R. C. *J. Am. Chem. Soc.* **2004**, *126*, 724−725. (c) Kapota, C.; Lemaire, J.; Maitre, P.; Ohanessian, G. *J. Am. Chem. Soc.* **2004**, *126*, 1836−1842. (d) Moore, D. T.; Oomens, J.; van der Meer, L.; von Helden, G.; Meijer, G.; Valle, J.; Marshall, A. G.; Eyler, J. R. *Chem. Phys. Chem.* **2004**, *5*, 740−743. (e) Moore, D. T.; Oomens, J.; Eyler, J. R.; Meijer, G.; von Helden, G.; Ridge, D. P. *J. Am. Chem. Soc.* **2004**, *126*, 14726−14727.
(9) Oepts, D.; van der Meer, A. F. G.; van Amersfoort, P. W. *Infrared Phys. Technol.* **1995**, *36*, 297−308.
(10) (a) Locke, M. J.; Hunter, R. L.; McIver, R. T. *J. Am. Chem. Soc.* **1979**, *101*, 272. (b) McLuckey, S. A.; Cameron, D.; Cooks, R. G. *J. Am. Chem. Soc.* **1981**, *103*, 1313−1317. (c) Meot-Ner, M. *J. Am. Chem. Soc.* **1984**, *106*, 1257−1264. (d) Price, W. D.; Schnier, P. D.; Williams, E. R. *J. Phys. Chem. B* **1997**, *101*, 664−673.
(11) (a) Price, W. D.; Jockusch, R. A.; Williams, E. R. *J. Am Chem. Soc.* **1997**, *119*, 11988−11989. (b) Wyttenbach, T.; Witt, M.; Bowers, M. T. *Int. J. Mass Spectrom.* **1999**, *182/183*, 243. (c) Strittmatter, E. F.; Wong, R. L.; Williams, E. R. *J. Phys. Chem. A* **2000**, *104*, 10271−10279. (d) Julian, R. R.; Hodyss, R.; Beauchamp, J. L. *J. Am. Chem. Soc.* **2001**, *123*, 3577−3583.
(12) Frisch, M. J.; Trucks, G. W.; Schlegel, H. B.; Scuseria, G. E.; Robb, M. A.; Cheeseman, J. R.; Zakrzewski, V. G.; Montgomery, J. A., Jr.; Stratmann, R. E.; Burant, J. C.; Dapprich, S.; Millam, J. M.; Daniels, A. D.; Kudin, K. N.; Strain, M. C.; Farkas, O.; Tomasi, J.; Barone, V.; Cossi, M.; Cammi, R.; Mennucci, B.; Pomelli, C.; Adamo, C.; Clifford, S.; Ochterski, J.; Petersson, G. A.; Ayala, P. Y.; Cui, Q.; Morokuma, K.; Malick, D. K.; Rabuck, A. D.; Raghavachari, K.; Foresman, J. B.; Cioslowski, J.; Ortiz, J. V.; Baboul, A. G.; Stefanov, B. B.; Liu, G.; Liashenko, A.; Piskorz, P.; Komaromi, I.; Gomperts, R.; Martin, R. L.; Fox, D. J.; Keith, T.; Al-Laham, M. A.; Peng, C. Y.; Nanayakkara, A.; Gonzalez, C.; Challacombe, M.; Gill, P. M. W.; Johnson, B.; Chen, W.; Wong, M. W.; Andres, J. L.; Gonzalez, C.; Head-Gordon, M.; Replogle, E. S.; Pople, J. A. *Gaussian 98*, revision A.9; Gaussian, Inc.: Pittsburgh, PA, 1998.
(13) Frisch, M. J.; Trucks, G. W.; Schlegel, H. B.; Scuseria, G. E.; Robb, M. A.; Cheeseman, J. R.; Montgomery, J. A., Jr.; Vreven, T.; Kudin, K. N.; Burant, J. C.; Millam, J. M.; Iyengar, S. S.; Tomasi, J.; Barone, V.; Mennucci, B.; Cossi, M.; Scalmani, G.; Rega, N.; Petersson, G. A.; Nakatsuji, H.; Hada, M.; Ehara, M.; Toyota, K.; Fukuda, R.; Hasegawa, J.; Ishida, M.; Nakajima, T.; Honda, Y.; Kitao, O.; Nakai, H.; Klene, M.; Li, X.; Knox, J. E.; Hratchian, H. P.; Cross, J. B.; Adamo, C.; Jaramillo, J.; Gomperts, R.; Stratmann, R. E.; Yazyev, O.; Austin, A. J.; Cammi, R.; Pomelli, C.; Ochterski, J. W.; Ayala, P. Y.; Morokuma, K.; Voth, G. A.; Salvador, P.; Dannenberg, J. J.; Zakrzewski, V. G.; Dapprich, S.; Daniels, A. D.; Strain, M. C.; Farkas, O.; Malick, D. K.; Rabuck, A. D.; Raghavachari, K.; Foresman, J. B.; Ortiz, J. V.; Cui, Q.; Baboul, A. G.; Clifford, S.; Cioslowski, J.; Stefanov, B. B.; Liu, G.; Liashenko, A.; Piskorz, P.; Komaromi, I.; Martin, R. L.; Fox, D. J.; Keith, T.; Al-Laham, M. A.; Peng, C. Y.; Nanayakkara, A.; Challacombe, M.; Gill, P. M. W.; Johnson, B.; Chen, W.; Wong, M. W.; Gonzalez, C.; Pople, J. A. *Gaussian 03*, revision B.5; Gaussian, Inc.: Pittsburgh, PA, 2003.
(14) Lin, C.; Oh, H.-B.; Hwang, H. Y.; Zhai, H.; Breuker, K.; Carpenter, B. K.; McLafferty, F. W., to be submitted.
(15) Wang, T.-C. L.; Ricca, T. L.; Marshall, A. G. *Anal. Chem.* **1986**, *58*, 2935−2938.

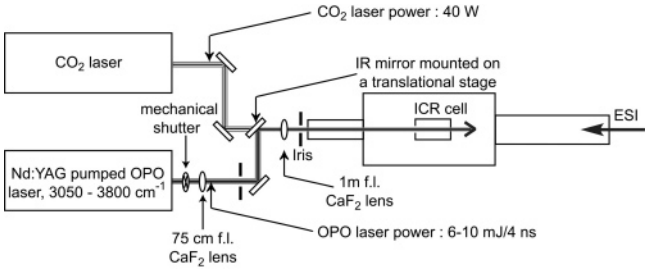


***Figure 2.*** Schematic of IRPD experimental configuration.

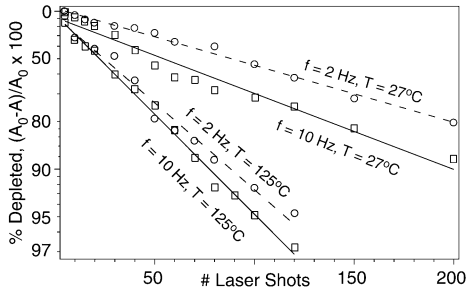


***Figure 3.*** $Gly_2H^+$ abundance depletion, plotted as $-\ln(A/A_0)$, as a function of the number of laser shots and laser operating repetition rates, and at two different cell temperatures. The OPO laser was tuned to 3584 $cm^{-1}$, and the output power was ~8 mJ per pulse.

(UNIBLITZ, Vincent Associates, Rochester, NY) just outside the laser exit, and the output laser power was varied by changing the delay between the flash lamp and Q-switch of the pump laser.

In a typical IRPD spectrum (Figure 1), the abundance $A$ of the precursor ions was measured in 5 nm steps, with the laser beam on ($A$) and off ($A_0$) for 15 s. The $A$ values were read directly from the Odyssey data acquisition system (Thermo-Finnigan) without apodization or zero-filling, correcting to a standard laser power of 10 mJ in 4 ns assuming a linear dependence.

Calculations were carried out at the B3LYP/6-31G(d) level of theory, as implemented in the Gaussian 98[12] and 03[13] suites of programs. Full geometry optimization was conducted at this level, although no attempt was made to search for all possible conformational minima, because that would be computationally prohibitive. Vibrational spectra were predicted from harmonic frequencies scaled by 0.97,[16] which in turn were derived from analytical Hessian calculations.

## Results and Discussion

**Photodissociation Mechanism.** For the previous IRPD spectra of ions,[2,3,8] dissociation was shown to result from resonant absorption that increased the ion's energy above the dissociation limit. In the previous ion flow systems (irradiation of a moving ion beam) used for the 2700−3900 $cm^{-1}$ spectra of weakly bound cluster ions,[3a−e] a ~1 mJ laser pulse caused the absorption of one or two photons per ion, sufficient for the <16 kcal/mol dissociation energy (3498 $cm^{-1}$ = 10 kcal/mol); however, no PD was observed for a dimer requiring ~21 kcal/mol.[3d] In our trapped ion experiments with the proton-bound glycine dimer ion (dissociation energy 27 kcal/mol),[10d] 200 pulses of ~8 mJ laser irradiation at the most intense spectral feature (3584 $cm^{-1}$) cause ~90% $Gly_2H^+$ depletion (Figure 3). At this resonant frequency, the value of $-\ln(A/A_0)$ (the ordinate plot of Figure 3) increases nearly linearly with the number of IR laser pulses. The laser pulse energy dependence is also linear with $-\ln(A/A_0)$ over the range studied (Figure 4); it would be

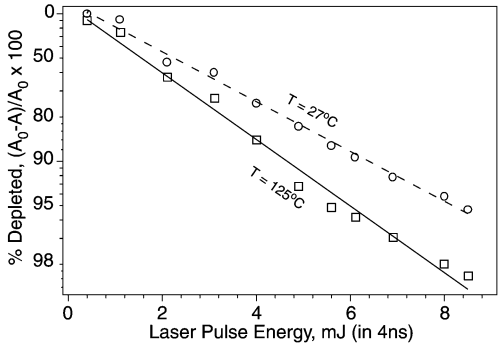


***Figure 4.*** $Gly_2H^+$ abundance depletion, plotted as $-\ln(A/A_0)$, as a function of laser pulse energy, 3584 $cm^{-1}$, 10 Hz repetition rate, cell 27 and 125 °C.

nonlinear with nonresonant absorption.[17] Absorption of a photon in a vibrational mode (pump mode) of the ion is followed by rapid (~$10^{-12}$ s) intramolecular energy redistribution into the other vibrational degrees of freedom of the ion.[1−3,17] The pump mode is then available to absorb a second photon within the same laser pulse, followed again by rapid energy distribution. This process is repeated until the internal energy exceeds the threshold sufficiently for dissociation to occur. Consistent with this, raising the temperature from 27 to 125 °C (Figures 3, 4) lowers the number of extra photons required. The excitation process is interrupted at the end of each 4 ns laser pulse, which should permit ion cooling,[18] and resumes when the next laser pulse comes in. Changing the delay between pulses from 0.1 to 0.5 s (Figure 3) decreases the extent of dissociation at both 27 and 125 °C, showing that cooling of the ions is incomplete after 0.1 s. Collisional cooling at the $10^{-9}$ Torr pressure should be unimportant, so that the cooling results from blackbody infrared radiation of the ions.[18] Note that ions dissociating 0.1−0.5 s after the laser pulse would actually increase the ion depletion for 2 versus 10 Hz. The power dependence (Figure 4) would not be linear if the excited $Gly_2H^+$ ions undergo substantial dissociation during the 4 ns laser pulse, as this would reduce the number of $Gly_2H^+$ ions available for resonant absorption, and thus reduce the overall absorption of additional photons.

**Peak Intensities in IRPD Spectra.** To produce the spectra of the amino acid dimers (Figure 1), the absorbed IR photons must cause dissociation of the noncovalent bonding. For an ion flow system, without ion storage, dissociation was not achieved for a dimer with a binding energy of ~21 kcal/mol.[3d] Binding energies of the symmetric proton-bound dimers of Gly, Ala, and Lys are ~27 kcal/mol,[10d] while those with $H^+$-binding between amine groups are 23 kcal/mol and those with $H^+$-binding between carbonyl groups are 31 kcal/mol.[10c,d] An attempt to obtain the IRPD spectrum of the pentapeptide ion $(Lys-Lys-Lys-Lys-Lys + 2H)^{2+}$ was unsuccessful, presumably because its covalent bond cleavage requires significantly more energy. IRPD was similarly unsuccessful for the complex $Cu^{II}[Ser_2(AcNH-Asp) - H]^+$. This results from fluence limitations of the OPO pulsed laser in the selected narrow frequency range; with higher power (25 W) the cw $CO_2$ laser

(16) Scott, A. P.; Radom, L. *J. Phys. Chem.* **1996**, *100*, 16502−16513.

(17) (a) Stannard, P. R.; Gelbart, W. M. *J. Phys. Chem.* **1981**, *85*, 3592−3599. (b) Green, D.; Hammond, S.; Keske, J.; Pate, B. H. *J. Chem. Phys.* **1999**, *110*, 1979−1989.

(18) (a) Price, W. D.; Schnier, P. D.; Williams, E. R. *Anal. Chem.* **1996**, *68*, 859. (b) Dunbar, R. C.; McMahon, T. B. *Science* **1998**, *279*, 194−197.

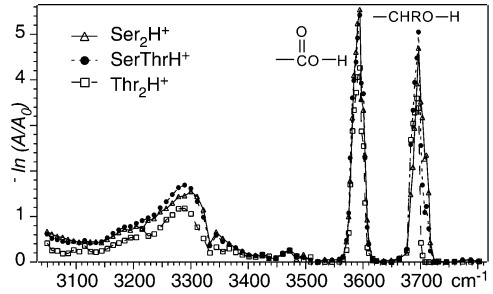


***Figure 5.*** IRPD spectra of $Ser_2H^+$, $Thr_2H^+$, and $SerThrH^+$; conditions of Figure 1.

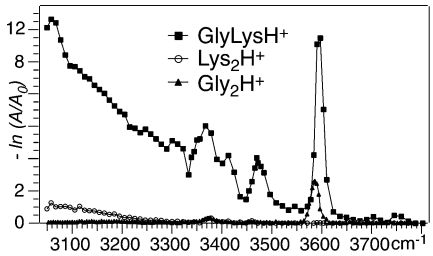


***Figure 6.*** IRPD spectrum of $GlyLysH^+$ versus those of $Gly_2H^+$ and $Lys_2H^+$; conditions of Figure 1.

(10.6 $\mu$m, Figure 2) easily causes nonresonant photodissociation of the $(Lys_5 + 2H)^{2+}$ peptide.[7] The free electron laser has a power of ~1 W (100 mJ in 0.1 s), but it is usually not operated at energies above 2100 $cm^{-1}$.[8,9]

Because IRPD produces an "action" spectrum, not a pure absorption spectrum, the absolute intensities of IRPD spectral peaks also depend on the number of IR photons required to raise the ion internal energy above the dissociation level. Most spectra of the amino acid protonated homodimers of Figures 1 and 5 show qualitatively similar intensities, reflecting their similar dissociation energies. However, the spectrum of the heterodimer $GlyLysH^+$ is far more intense than that of either $Gly_2H^+$ or $Lys_2H^+$ (Figure 6). Consistent with this, the dissociation energies of amino acid $H^+$ dimers decrease linearly with the difference in the proton affinities of the components.[10c] Because of the dissociation energy effect on the extent of molecular ion dissociation, the discussion below considers the absorptivity at a specific frequency relative to that at other frequencies in that spectrum, not those in other spectra.

**Functional Group Effects.** The early 925−1090 $cm^{-1}$ IRPD spectra of gaseous ions formed by electron ionization[2] were found to be similar to the IR absorption spectra of the corresponding neutrals.[19] Here, particular frequencies of absorbed IR photons leading to photodissociation of the gaseous proton-bound amino acids from 22 IRPD spectra are also correlated directly with solution-observed O−H and N−H stretching frequencies, the major functional groups responding in the 3050−3800 $cm^{-1}$ region.[19] These bonds are weakened, and the frequencies are lowered (red shifted), by hydrogen bonding and by an electron-withdrawing group or a partial positive charge on the heteroatom. In the spectra of small gaseous proton-bound cluster ions,[3] both the observed and the theoretically calculated frequencies were found to be 50−75 $cm^{-1}$ higher (blue shifted) than those of the neutrals in solution.

The three serine and threonine dimer spectra show a prominent 3697 $cm^{-1}$ peak (Figure 5) whose value is blue shifted versus the 3590−3650 $cm^{-1}$ strong absorptions found in solution for the free aliphatic hydroxyl O−H stretching frequencies.[19] The Figure 5 spectra also show a broad peak maximized at 3300 $cm^{-1}$ that should correspond to weakening of aliphatic and/or carboxylic O−H groups by hydrogen bonding of the H atom; a very similar peak is present in the spectra of [(D or L)-Ser−(L-Asp)]$H^+$.[20] In solution spectra of aliphatic alcohols, intermolecular hydrogen bonding between hydroxyl groups produces a broad absorption centered around 3300 $cm^{-1}$.[19]

The Figure 5 and other IRPD spectra show strong absorptions at ~3590 $cm^{-1}$, somewhat blue shifted versus those of ~3520 $cm^{-1}$ found in solution for the free carboxyl O−H group;[19] the electron-withdrawing carbonyl group has red shifted the aliphatic O−H absorption by ~100 $cm^{-1}$. Carboxyl methylation in (α-AcNH−Lys−OMe)$_2H^+$ (Figure 1C) removes the 3590 $cm^{-1}$ peak. For $(AcNH-Asp)_2H^+$ (Figure 1B), hydrogen-bonding red shifts one carboxyl O−H absorption to 3425 $cm^{-1}$, with even more extensive red shifting in the spectrum of $Lys_2H^+$ (Figure 1D). The gaseous octamer L-$Ser_8H^+$ appears to have exciting chiral selectivity;[21] the IRPD spectrum of it and its racemate show a similar strong absorption at 3425 $cm^{-1}$, but no peaks at 3695, 3590, or 3300 $cm^{-1}$.

For primary amines in solution, the free N−H symmetric and asymmetric stretches are at ~3400 and ~3500 $cm^{-1}$, respectively, but are weak;[19] their gaseous counterparts are weak and difficult to assign without theory. A partial positive charge on the nitrogen red shifts the absorption and increases the absorptivity; theory assigned the 3375 $cm^{-1}$ peak in the spectrum of $NH_4^+(H_2O)_3$ to the free $N^{+-}H$ stretch.[3b] In the $Gly_2H^+$ spectrum (Figure 1A), the 3375 $cm^{-1}$ peak corresponds to the symmetric −HN(−$H^+$)−H stretch, with the neutral −HN−H stretch peaks much weaker.

In solution, the primary and secondary amide stretch peaks are at 3400−3500 $cm^{-1}$, but are "moderately intense".[19] The gaseous formamide complex $NH_4^+[HC(=O)NH_2]_3$ gives prominent symmetric and asymmetric amide N−H stretches at 3436 and 3554 $cm^{-1}$.[3d] The strong 3440 $cm^{-1}$ absorption in (α-AcNH−Lys−OMe)$_2H^+$ (Figure 1C) should represent an amide free N−H stretch; it is weaker in Lys(α-AcNH−Lys−OMe)-$H^+$ and negligible in the underivatized $Lys_2H^+$ (Figure 1D). However, the apparently similar 3440 $cm^{-1}$ peak in (α-AcNH−Lys−OMe)(AcNH−Asp)$H^+$ (Figure 1E) corresponds to 3455 $cm^{-1}$ peaks in the (D- or L-Lys)(L-AcNH−Asp)$H^+$ spectra and 3465 $cm^{-1}$ peaks in the (D- or L-Lys)(L-Asp)$H^+$ spectra,[20] and the last has no amide functionality. All of these $Lys_2AspH^+$ spectra also have 3370 $cm^{-1}$ peaks that must also arise from underivatized carboxy or $-NH_2$ groups that are hydrogen bonded or N-protonated.

However, all 12 spectra of complexes that contain lysine have dominant broad absorptions below 3150 $cm^{-1}$, as do the spectra of the L- and racemic $Ser_8H^+$.[20] The extra $\epsilon$-$NH_2$ group of lysine is at the end of a long flexible chain and has a far higher proton

(19) Silverstein, R. M.; Webster, F. X. *Spectrometric Identification of Organic Compounds*; Wiley: New York, 1998; pp 87−104.

(20) The effects of amino acid chirality on IRPD spectra will be discussed in a later publication.

(21) (a) Hodyss, R.; Julian, R. R.; Beauchamp, J. L. *Chirality* **2001**, *13*, 703−706. (b) Cooks, R. G.; Zhang, D.; Koch, K. J.; Gozzo, F. C.; Eberlin, M. N. *Anal. Chem.* **2001**, *73*, 3646−3655. (c) Takats, Z.; Nanita, S. C.; Schlosser, G.; Vekey, K.; Cooks, R. G. *Anal. Chem.* **2003**, *75*, 6147−6154.

affinity than any other structural functionality in the proton-bound complexes studied here (complexes containing the other basic amino acids, arginine[1b,11] and histidine, have not been examined as yet). In solution IR spectra, intermolecular hydrogen bonding of the neutral amines and amides does not red shift the neutral N−H absorption as far as 3150 $cm^{-1}$. Farther shifts in solution are only found for charged nitrogen species in which the $N^+$−H must be involved in extensive intermolecular hydrogen bonding.[19] This results in a broad, prominent stretching band in the 2600−3100 $cm^{-1}$ region of amino acids in solution,[19] where they are known to exist as zwitterions.[10,11] In the IRPD spectra of gaseous cluster ions, similar prominent absorption bands representing hydrogen-bonded $N^+$−H stretching vibrations (even without zwitterion formation) are found in the 2900−3250 $cm^{-1}$ region of the $NH_4^+(H_2O)_n$, $n = 3-6$, and $NH_4^+[HC(=O)NH_2]_3$ ions.[3b,d] The cluster ions $H^+(H_2O)_n$, $n = 5-8$, and $H^+(CH_3OH)(H_2O)_n$, $n = 2-6$, show less or no absorption in this region.[3c,e] Thus, the prominent absorptions below 3150 $cm^{-1}$ in these IRPD spectra of ions that contain lysine should represent $N^+$−H groups with strong hydrogen bonding, for which the $\epsilon$-$NH_2$ group of lysine is favored because of its high proton affinity and ability to H-bond to remote heteroatoms through its flexible $-(CH_2)_4-$ linkage. Supporting the $\epsilon$-$NH_2$ assignment, this absorption below 3150 $cm^{-1}$ is not appreciably affected by acetylation on the α-$NH_2$ groups in the IRPD spectra of (α-AcNH−Lys−OMe)$_2H^+$ (Figure 1C), (α-AcNH−Lys−OMe)(AcNH−Asp)-$H^+$ (Figure 1E), or (α-AcNH−Lys−OMe)$_2$(AcNH−Asp)$H^+$ (Figure 1F). However, absorption below 3150 $cm^{-1}$ is not definitive for hydrogen-bonded $N^+$−H; carboxylic acid solution dimers give an intense, broad O−H stretch at 2500−3300 $cm^{-1}$, centered near 3000 $cm^{-1}$,[19] and the $Ser_8H^+$ absorptions are increasingly the most intense below 3200 $cm^{-1}$.[20] Further, absorptions of amine salts in solution can be red shifted below this region, with HRR′$N^+$−H at 2700−3000 $cm^{-1}$ and RR′R″$N^+$−H at 2250−2700 $cm^{-1}$.[19] The H-bonding distances and angles in such dynamic species vary continuously over a considerable range, producing this substantial broadening of the absorption bands,[3,19] while charging at the N−H bond produces a far greater change in dipole moment on stretching, leading to far higher absorptivities.

Aliphatic C−H stretching bands in solution are almost always in the 2840−2975 $cm^{-1}$ region; with gas-phase blue shifting, these could only be at the low end of our frequency range where Figure 1A,B shows no appreciable absorption. As was found to be of critical value in interpreting the spectra of small gaseous species,[1,3] we turn to theory to clarify these preliminary correlations.

**Theoretical Predictions of Conformations and IRPD Spectra.** Dimer conformations and vibrational frequencies were predicted by B3LYP/6-31G(d) DFT calculations (Figures 7−10).[12,13] These are a reasonable compromise between accuracy and calculation time for such relatively large molecules. The calculated frequencies were scaled by 0.97:[16] a factor of 0.976 was found optimum in previous studies in the 2700−3900 $cm^{-1}$ region.[3]

However, for the $(H_2O)_2H^+$ absorptions in the 800−1500 $cm^{-1}$ region, serious errors in frequency prediction appear to be due to anharmonic effects.[8a,d] To assess whether the conventional scaling[8a,d] of harmonic frequencies would correct

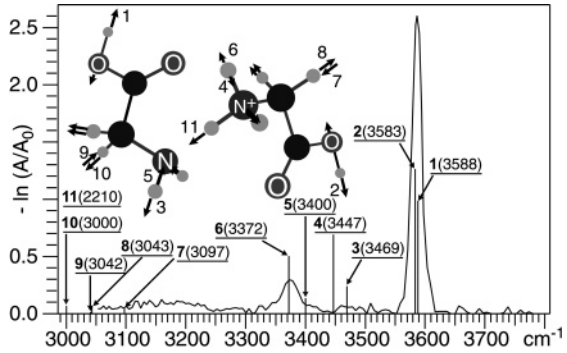


***Figure 7.*** Comparison of the experimental IRPD spectrum (solid lines) of $Gly_2H^+$ to that predicted by theory (vertical bars). The predicted most intense peak at 2210 $cm^{-1}$ (#7, not shown) corresponds to the asymmetric stretch of the N−$H^+$···N of the ionic hydrogen-bonding moiety.

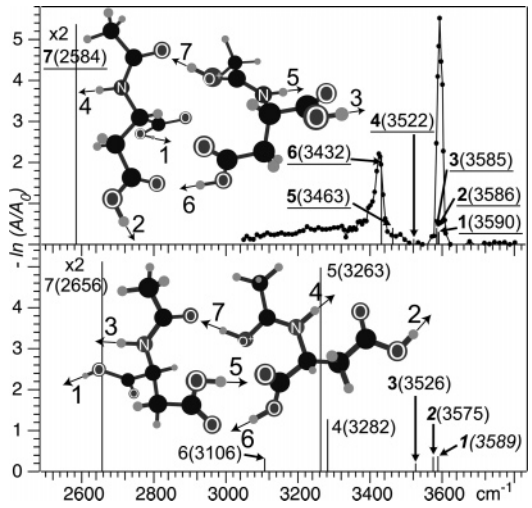


***Figure 8.*** Comparison of the experimental IRPD spectrum (top right) of $(AcNH-Asp)_2H^+$ and those predicted by theory for the two lowest energy conformers.

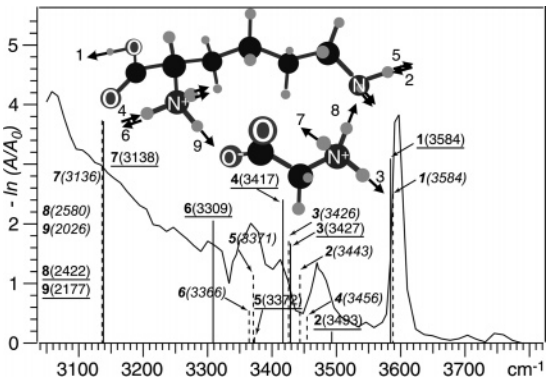


***Figure 9.*** Comparison of the experimental IRPD spectrum of $GlyLysH^+$ and those predicted by theory. Lowest energy conformer (shown), vertical solid lines; alternative zwitterion conformer protonated instead at the Lys $\epsilon$-$NH_2$ group, vertical dashed lines, with bond designations and frequencies in italics.

for anharmonicities in the present examples, an anharmonic spectrum was computed at the MP2/6-311G(d,p) level for the proton-bound dimer of ammonia, using the PT2-VSCF method,[22] as implemented in GAMESS.[23] The results are summarized in Table 1.

The N−H stretches are modes 1−7 in Table 1. One sees that for six of these modes, multiplication of the harmonic frequency

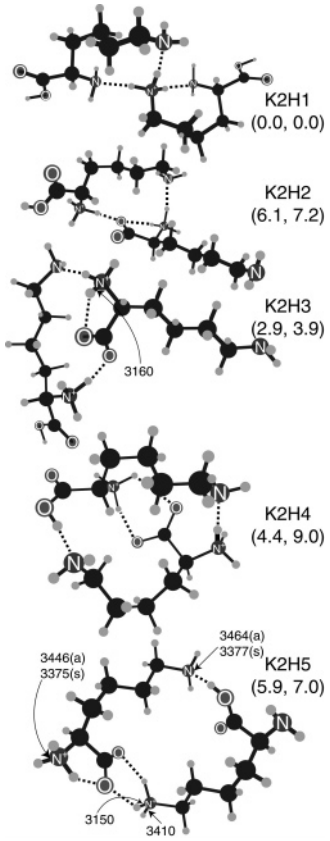


***Figure 10.*** Predicted structures and selected IRPD frequencies of five $Lys_2H^+$ isomers; predicted relative values of $\Delta H°$ and $\Delta G°$ in parentheses.

***Table 1.*** Harmonic and Anharmonic (PT2-VSCF) Vibrational Frequencies (in $cm^{-1}$) for the $C_{3v}$ Proton-Bound Dimer of Ammonia

| mode | harmonic | PT2-VSCF |
|---|---|---|
| 1 | 3613.75 | 3335.41 |
| 2 | 3613.75 | 3298.22 |
| 3 | 3592.41 | 3335.98 |
| 4 | 3592.41 | 3307.01 |
| 5 | 3493.36 | 3294.83 |
| 6 | 3474.53 | 3274.28 |
| 7 | 1849.86 | 577.21 |
| 8 | 1780.49 | 1711.22 |
| 9 | 1780.49 | 1710.87 |
| 10 | 1662.68 | 1626.87 |
| 11 | 1662.68 | 1604.31 |
| 12 | 1592.58 | 1554.03 |
| 13 | 1592.58 | 1548.05 |
| 14 | 1377.98 | 1383.35 |
| 15 | 1309.12 | 1498.31 |
| 16 | 613.84 | 733.01 |
| 17 | 613.84 | 725.61 |
| 18 | 393.88 | 485.69 |
| 19 | 393.88 | 497.13 |
| 20 | 325.54 | 423.46 |
| 21 | 0.20 | 0.03 |

by a constant factor (in this case, 0.928) would do a reasonable job of correcting for anharmonicity. However, for mode 7 that is clearly not the case. Mode 7 is the stretching of the N−H bond to the hydrogen that is on the three-fold axis, that is, is hydrogen bonded from the ammonium ion to the neutral ammonia. The reason for its enormous anharmonicity is easy to understand when one calculates the $D_{3d}$ transition state for proton transfer. It sits only 0.55 kcal/mol higher in potential energy than the $C_{3v}$ minimum. This places the barrier to proton transfer below even the zero-point energy of the anharmonic stretching mode. Thus, mode 7 is very like the reaction coordinate for proton transfer. The calculation of the PT2-VSCF frequencies of the proton-bound ammonia dimer took more than 1500 times longer than the calculation of its harmonic spectrum, and so it is apparent that application of this procedure to larger systems is not feasible. However, we think that the lessons learned from this model calculation can be transferred to the systems of interest in the present paper.

In the computed spectra of the proton-bound amino acid pairs, most of the IRPD absorptions in the range 3050−3800 $cm^{-1}$ correspond to stretching of the bond to an "unshared" hydrogen atom. Consequently, the calculated harmonic frequencies, when corrected by the scale factor appropriate to the method, should provide a reasonable fit to experiment. By contrast, the harmonic frequency of a stretching motion for a hydrogen atom "shared" between an ammonium ion and an amine is probably a unreliable predictor of the real IRPD absorption position for such modes. Similarly, hydrogens acting as intermolecular bridges between an ammonium ion and a carboxylate ion are likely to have very anharmonic stretches whose frequencies cannot be reliably predicted by harmonic approximation. Most of these modes have computed harmonic frequencies below 3000 $cm^{-1}$ and so are outside of our IRPD spectral window. An exception is the N−H stretch in Figure 9 predicted to have a harmonic frequency of 3138 $cm^{-1}$.

Less is known about the factors that affect the accuracy of the calculated IRPD absorptivities, which represent peak areas, not intensities. As was found in previous studies[3,8] as well as here, disagreement between theoretical and experimental absorptivities can be far greater than that from peak area uncertainties.

**$Gly_2H^+$.** Calculations for the proton-bound glycine dimer were based on the minimum energy structure deduced by Williams' MP2/3-21G* calculations.[10d] The resulting lowest energy conformer (Figure 7) has a similar proton-bonding between the two amino groups and a calculated dissociation energy of 32.6 kcal/mol versus 27 kcal/mol measured.[10d] The dominant experimental peak at ~3584 $cm^{-1}$ corresponds to the two unbound carboxyl O−H stretches (#1, 2, predicted 3583 and 3588 $cm^{-1}$). Consistent with such a doublet, full width at half-maximum (fwhm) is 20 $cm^{-1}$, with ~5 $cm^{-1}$ due to the line width of the employed IR radiation, plus the various rotational transitions within the same vibrational manifold (note the narrower 3590 $cm^{-1}$ peak in Figure 1E). The #6, 3372 $cm^{-1}$ prediction of an unbound symmetric amine $N^+$−H stretch corresponds to the next most intense peak, with the #5 symmetric N−H explaining its 3400 $cm^{-1}$ shoulder. The corresponding asymmetric stretches (#4, #3) in the 3425−3550 $cm^{-1}$ region, although predicted to be even more intense, are of low signal/noise; the symmetric/asymmetric intensity ratio has also been predicted poorly in some (not all) previous studies.[3] Note that if the carboxyl O−H groups are unbound, there are no obvious alternatives to the $N^+$−H assignment as

(22) (a) Chaban, G. M.; Jung, J. O.; Gerber, R. B. *J. Chem. Phys.* **1999**, *111*, 1823−1829. (b) Matsunaga, N.; Chaban, G. M.; Gerber, R. B. *J. Chem. Phys.* **2002**, *117*, 3541−3547. (c) Chaban, G. M.; Xantheas, S. S.; Gerber, R. B. *J. Phys. Chem. A* **2003**, *107*, 4952−4956.
(23) GAMESS Version 12 DEC 2003 (R1): Schmidt, M. W.; Baldridge, K. K.; Boatz, J. A.; Elbert, S. T.; Gordon, M. S.; Jensen, J. J.; Koseki, S.; Matsunaga, N.; Nguyen, K. A.; Su, S.; Windus, T. L.; Dupuis, M.; Montgomery, J. A. *J. Comput. Chem.* **1993**, *14*, 1347−1363.

the 3375 $cm^{-1}$ peak; if this peak represents the asymmetric stretch, the expected symmetric stretch at ~3300 $cm^{-1}$ is not obvious. The calculated C−H stretch vibrations in the 3000−3100 $cm^{-1}$ region are of similarly low intensity.

The conformer calculated by Williams is closely similar,[10d] except that the charge on the protonated amino group is "solvated" by the carboxyl oxygen of the same amino acid as well as the amine nitrogen of the other acid. The resulting red shifting of N−H stretch peaks could produce the observed weak absorptions in the 3100−3230 $cm^{-1}$ region, so that the IRPD spectrum may also give evidence for some additional presence of the Williams conformer.[10d]

The strongest (×10) peak predicted by theory at ~2200 $cm^{-1}$ (#11), corresponding to the stretching of the N···$H^+$···N ionic hydrogen bond, is outside the range of our OPO laser. For its deuterated analogue, $Gly_2D^+$, the first overtone of N···$D^+$···N should be at 2210 × 2 (overtone)/1.414 (reduced mass) ≈ 3125 $cm^{-1}$. Unfortunately, the 3050−3800 $cm^{-1}$ IRPD spectrum of $Gly_2D^+$ showed no signals above noise, even with 32 s laser on-time. Very recently, Asmis and co-workers have reported the gas-phase IRPD spectra of the jet-cooled protonated water dimer ion $(H_2O)_2H^+$ and its deuterated analogue using an MS/MS ion trap and free electron laser.[8a] However, their theoretical calculations were able to identify the stretching and bending vibrational bands associated with this ionic hydrogen-bonding moiety O···$H^+$···O only with extensive corrections for anharmonic effects. As discussed above, these effects should also modify our prediction for the N···$D^+$···N frequency.

**(AcNH−Asp)$_2$H$^+$.** Theoretical calculations for the amine-acylated aspartic acid dimer gave two lowest energy conformers (Figure 8), with the bottom one 2 kcal/mol higher in energy. Their calculated binding energies of ~39 kcal/mol are ~6 kcal/mol higher than that calculated here for $Gly_2H^+$, consistent with proton bonding between the amide carbonyl groups; symmetric dimers proton-bound at carbonyls typically have ~8 kcal/mol higher binding energies than those containing amine protonation[10c] (however, this decrease in $Gly_2H^+$ binding energy should increase its tendency for photodissociation, which is not reflected in the relative peak intensities of Figure 7 vs 8, vide supra). Although the calculated frequencies for the free COO−H groups of both conformers are in satisfactory agreement with that of the dominant 3590 $cm^{-1}$ peak, otherwise the conformers have dramatically different predicted spectra (Figure 8). In conformer 1, the O−H of one $\beta$-carboxyl is H-bonded to the carbonyl of the other $\beta$-carboxyl, (O═)CO−H···O═C(OH), whose predicted frequency of 3432 $cm^{-1}$ matches that of the next most intense ~3425 $cm^{-1}$ peak in the spectrum. In conformer 2, the $\alpha$-carboxyl group of the protonated acid and the $\beta$-carboxyl of the other acid are held together by two such H-bonds. This should produce far greater red shifts for these O−H groups; the predicted absorptions at 3106 and 3263 $cm^{-1}$ are not evident in the spectrum (in solution, such carboxylic acid dimers give a broad absorption 2500−3300 $cm^{-1}$).[19] Less intense absorptions are predicted for the (Ac)N−H stretch frequencies; for conformer 1, these (#5, 4) are at 3463 (some actual absorption) and 3522 (in the noise) $cm^{-1}$, but for conformer 2, they are at (#4, 3) 3282 and 3526 $cm^{-1}$ (both in the noise). The IRPD spectrum clearly indicates structure 1 as the predominant conformer.

**GlyLysH$^+$.** Theoretical calculations for the glycine/lysine heterodimer predicted two similar lowest energy isomers, with glycine as a zwitterion in both.[1b,11] The Figure 9 isomer is favored by 2 kcal/mol, while isomer 2 is protonated instead on the $\epsilon$-$NH_2$ group of lysine, which is coordinated to the carboxylate anion of the zwitterionic glycine. The predicted frequencies (isomers 1 and 2, solid and dashed vertical lines, respectively) give support to the isomer 1 structure with the 3309 $cm^{-1}$ $N^+$−H prediction, to isomer 2 with the 3366 $N^+$−H and 3371 N−H $cm^{-1}$ predictions, with both supported by the 3136, 3138, 3417, 3426, and 3427 $cm^{-1}$ $N^+$−H predictions. The experimental 3475 $cm^{-1}$ peak is predicted only marginally by either. Thus, both isomers may well be present, with the extensive broad absorptions below 3200 $cm^{-1}$ due to the dynamic variation in bond length and angles for the ammonium hydrogen bonding.

As discussed above, frequency predictions #8 and #9 should be subject to substantial anharmonic effects. However, for the intramolecular bridging hydrogen between the ammonium ion and the carboxylate of a zwitterionic glycine (#7), the harmonic frequency of 3138 $cm^{-1}$ found in the B3LYP calculations should be affected minimally by anharmonicity. Calculations show that the complete transfer of this hydrogen (while keeping all other atoms fixed) raises the potential energy of the complex by 23 kcal/mol. Consequently, the stretching of the N−H bond does not correspond to the reaction coordinate for a low-barrier proton transfer and should therefore not be unusually anharmonic. For the predicted strong absorption, there is a corresponding increase with lowered frequencies near 3138 $cm^{-1}$, but no discernible peak. Stabilization of the gaseous glycine zwitterion has been achieved, overcoming the ~20 kcal/mol barrier[10a] versus its gaseous neutral form.

**Lys$_2$H$^+$.** The largest species subjected to theoretical calculations was the lysine dimer. Here, theory appears to be inadequate; the predicted structure of lowest energy (K2H1, Figure 10) contains two free carboxyl O−H groups, while any absorption in the −COO−H stretch region of ~3590 $cm^{-1}$ for the three $Lys_2H^+$ derivatives is clearly in the noise level (Figure 11). This is also true for the Lys($\alpha$-AcLys−OMe)$H^+$ and ($\alpha$-AcLys−OMe)$_2H^+$ dimer spectra. The zwitterionic structure is favored for the GlyLys$H^+$ dimer, but the calculated $Lys_2H^+$ isomers containing this feature (K2H2 and K2H3, Figure 10) not only are of higher energy, but also still contain a free carboxyl O−H group. These isomers have an extended aliphatic chain terminated with the $\epsilon$-$NH_2$ group; hydrogen bonding this free $\epsilon$-$NH_2$ to the free carboxyl O−H (K2H4, Figure 10) removes the predicted ~3190 $cm^{-1}$ peak, but gives an isomer of high free energy. The strain is somewhat lowered by H-bonding of each $\epsilon$-$NH_2$ to their counterpart carboxyls (K2H5), with one such bonding involving a zwitterion, but its $\Delta H$ is still predicted to be 5.9 kcal/mol higher than that of K2H1. It appears that this level of theory is inadequate for this large system with numerous H-bonding functionalities.

Despite these limits of theory, the experimental IRPD spectra of Figure 11 do provide evidence of the structure of $Lys_2H^+$, such as absence of free carboxyl groups. The free N−H stretches are weak and at frequencies similar to those of the $Gly_2H^+$ spectrum. Note the more intense 3440 $cm^{-1}$ that appears with acetylation of one or both $\alpha$-$NH_2$ groups of the lysines. This acetylation has little effect on the rest of the spectrum, consistent

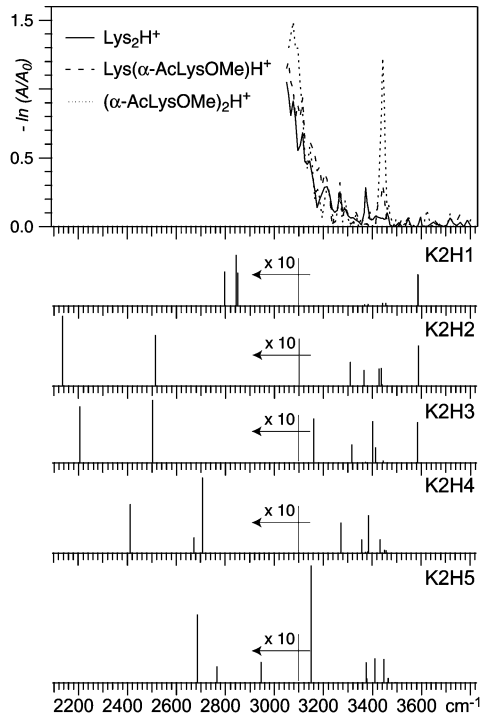


***Figure 11.*** Comparison of the experimental IRPD spectra of $Lys_2H^+$ (top, solid line), $(\alpha\text{-AcNH}-Lys-OMe)_2H^+$ (dotted line), and $Lys(\alpha\text{-AcNH}-Lys-OMe)H^+$ and those predicted by theory for $Lys_2H^+$ (Figure 10). The three spectra were measured at the same time, more than 1 year later than those of Figure 1.

with zwitterionic bonding of the $\epsilon$-$NH_2$ and carboxy groups causing the strong absorption below 3200 $cm^{-1}$. This region is also nearly featureless in the other spectra examined here, including those of $Ser_8H^+$.

It is unclear at this stage whether the global free-energy minimum for the proton-bound lysine dimer corresponds to an isomer that has not been considered, or whether the computed relative energies of the isomers described above are simply in error. There are large spectral differences predicted for the 2150−3050 $cm^{-1}$ region, so that extension of the IRPD spectral range could be useful.

**Specific IR Photodissociation for Gaseous Ion Reaction Studies.** IRPD spectra can also provide a uniquely specific method for identification and measurement of an isomeric product of a gaseous ion reaction. For example, the characteristic 3700 $cm^{-1}$ peak of the $Ser_2H^+$ dimer (Figure 5) would clearly distinguish it from an isomeric product without a free aliphatic hydroxyl group.[21]

The frequency selectivity of IRPD should also be useful for photodissociation of specific gaseous ions, such as to avoid the secondary dissociation of reaction products. To distinguish between charge-solvation ($ABBH^+$) and salt bridge ($BABH^+$) structures of trimers of trifluoroacetic acid (AH) and organic bases (B), Williams and co-workers measured the relative amounts of $B_2H^+$ and $BH^+$ formed by blackbody IR photodissociation.[11c] Because $BH^+$ is also formed by secondary dissociation of $B_2H^+$, its measurement required simultaneous resonant ejection of the $B_2H^+$ ions with a continuous rf waveform. Although no primary $ABH^+$ ions were formed to cause interference, measurement of the primary $B_2H^+$ product is compromised by its secondary dissociation. In comparison, IRPD at room temperature of $(\alpha\text{-AcNH}-Lys-OMe)_2(AcNH-Asp)H^+$ trimer at 3500 $cm^{-1}$, where the absorption cross sections of the dimers $(\alpha\text{-AcNH}-Lys-OMe)(AcNH-Asp)H^+$ and $(\alpha\text{-AcNH}-Lys-OMe)_2H^+$ are minimal (Figure 1C,E,F), gave the latter as the dominant product. However, dissociation of the trimer at 3448 $cm^{-1}$, where both dimer products have strong absorptions, dramatically increased formation of the monomer $(\alpha\text{-AcNH}-Lys-OMe)H^+$.

## Conclusions

Electrospray ionization has now been used to provide abundant molecular ions for IRPD spectra of relatively high quality over the tunable 3050−3800 $cm^{-1}$ range of an OPO laser. The long ion storage capability of the FTMS instrument provides high detection sensitivity, so that spectra were obtained from ions whose photodissociation required up to 40 kcal/mol, more than double the upper limit of the previous flow IRPD methods.[3] Peak frequencies of these gaseous ion spectra agree generally with correlations established for solution IR spectra of neutrals. Comparison of experimental IRPD spectra of $Gly_2H^+$, $(AcNH-Asp)_2H^+$, and $GlyLysH^+$ dimer ions with those predicted by theory provides structural information for identifying the lowest energy conformation. This comparison also provides direct references for the red shifting of O−H and N−H absorption peaks and for peak widths caused by H-bonding and heteroatom charging. For the largest dimer studied, $Lys_2H^+$, theory found no low energy structure consistent with the IRPD spectrum, a challenge for future theoretical studies. Although absorptivity predictions can be poorly reliable, IRPD appears promising as a complementary method for the structural characterization of gas-phase ions; applications to multiply charged protein ions[5] will be demonstrated in a later paper.[14]

**Acknowledgment.** We thank Floyd Davis, Tadhg Begley, Xuemei Han, and Foil Miller for helpful discussions and the National Institutes of Health (Grant GM 16609) for generous financial support.

JA040136N